Journal of Carcinogenesis
Covering Genesis to Therapeutics

Journal of Carcinogenesis, ISSN: 1477-3163
2025; Vol 24: Issue 4s, https://carcinogenesis.com/

Biogenic Silver Nanoparticles Co-Loaded with Curcumin and Folic Acid: A Synergistic Approach for Breast Cancer Therapy

Runa Chakravorty[1], Bipul Nath[1*], Pranabesh Sikdar[1], Neelakshi Sharma[1], Moidul Islam Judder[1], Himanta Biswa Saikia[1], Manas Jyoti Kapil[2], Charu Chandrakant Mehta[3]

[1]Department of Pharmacy, Royal School of Pharmacy, The Assam Royal Global University, Betkuchi, Guwahati, Assam-781035, India

[2]Institute of Pharmacy, Assam Don Bosco University, Tapesia Gardens, Sonapur, Assam-782402, India

[3]School of Pharmaceutical Sciences, Faculty of Health Sciences, J.S.P.M. University, Wagholi, Pune, Maharashtra, India

Corresponding authors'

Prof. (Dr.) Bipul Nath,

Professor, Royal School of Pharmacy, The Assam Royal Global University, Guwahati, Assam- 781035, India.

Email ID : bipulnath@gmail.com

ABSTRACT

Breast cancer remains a major cause of cancer-related mortality worldwide, underscoring the need for targeted and effective therapeutic strategies. This study presents the biogenic synthesis of silver nanoparticles (AgNPs) using Houttuynia cordata extract as a reducing and stabilizing agent, followed by curcumin (Cur) loading and folic acid (FA) functionalization for selective breast cancer therapy. The nanoparticles were characterized via UV–Vis spectroscopy, FTIR, dynamic light scattering (DLS), scanning electron microscopy (SEM), and transmission electron microscopy (TEM), confirming nanoscale formation, stability, and morphology. Zeta potential analysis demonstrated enhanced colloidal stability, while FTIR verified biomolecular binding. Curcumin, a potent anticancer compound with poor bioavailability, was efficiently encapsulated, and FA conjugation enabled targeted delivery to folate receptor-overexpressing breast cancer cells. FA-Cur-AgNPs exhibited improved stability, higher cellular uptake, and greater selective cytotoxicity against MCF-7 cells compared to free Cur or AgNPs alone. MTT assay revealed significant dose-dependent cytotoxicity (IC_{50} = 5313.34 ppm), and AO/EtBr staining confirmed apoptosis induction. The formulation also displayed pH-responsive drug release, facilitating controlled delivery in the tumor microenvironment. These findings suggest that FA-functionalized, curcumin-loaded biogenic silver nanoparticles (FA-Cur-Hc-AgNPs) represent a promising green nanotherapeutic platform, enhancing drug bioavailability, selectivity, and anticancer efficacy while minimizing systemic toxicity.

Keywords: *Biogenic silver nanoparticles, Houttuynia cordata, curcumin, folic acid, targeted therapy, breast cancer, apoptosis, pH-responsive drug release.*

How to Cite: Runa Chakravorty, Bipul Nath, Pranabesh Sikdar, Neelakshi Sharma, Moidul Islam Judder, Himanta Biswa Saikia, Manas Jyoti Kapil, Charu Chandrakant Mehta, (2025) Biogenic Silver Nanoparticles Co-Loaded with Curcumin and Folic Acid: A Synergistic Approach for Breast Cancer Therapy, *Journal of Carcinogenesis*, *Vol.24, No.4s*, 632-643

1. INTRODUCTION

Cancer remains a major global health challenge, with over 20 million new cases and 10 million deaths annually. The global burden of cancer is projected to reach 28 million cases by 2040, emphasizing the need for improved therapeutic strategies. Among the most prevalent malignancies, breast cancer accounted for approximately 2.3 million new cases worldwide in 2020, making it the most frequently diagnosed cancer, according to the World Health Organization (WHO). Breast cancer primarily affects adolescent and middle-aged women, with its incidence and mortality rates rising steadily. Various factors contribute to this increasing trend, including early onset of menstruation, delayed menopause, obesity, hormone replacement therapy, sedentary lifestyles, and reduced breastfeeding practices [1]. Conventional treatment approaches such as chemotherapy, radiotherapy, and surgical intervention remain the primary options for breast cancer management. However, these treatments often pose significant challenges, including systemic toxicity, suboptimal drug delivery, and

poor drug stability, necessitating the development of innovative therapeutic strategies [2].,

Nanotechnology has emerged as a revolutionary approach in cancer treatment, leading to the field of cancer nanomedicine. Among the various nanomaterials, silver nanoparticles (AgNPs) have garnered significant interest due to their unique biomedical applications. AgNPs exhibit remarkable physicochemical properties, including antimicrobial, anti-inflammatory, and anticancer activities [3,4]. The biosynthesis of AgNPs is gaining prominence due to its eco-friendly nature and potential for sustainable material synthesis. Biogenic synthesis of AgNPs using plant extracts provides an alternative to chemical and physical methods, ensuring enhanced biocompatibility and stability. Houttuynia cordata (H. cordata), a medicinal plant with known anticancer potential, serves as an excellent biological source for the biogenic synthesis of AgNPs. The bioactive compounds present in H. cordata act as reducing and stabilizing agents during AgNP synthesis, enhancing nanoparticle stability while providing a cost-effective and environmentally sustainable production method [5,6].

Utilizing biological sources such as plants, fungi, and bacteria, the biogenic synthesis of silver nanoparticles offers an eco-friendly and widely preferred approach to nanoparticle production. Biogenic synthesis provides several advantages over conventional methods, including lower toxicity, cost-effectiveness, and environmental sustainability [7]. Plant-derived bioactive compounds have been extensively studied for their potential anticancer properties, as they can inhibit, slow down, or even reverse cancer cell proliferation. However, these phytochemicals often face challenges such as limited solubility, low bioavailability, and lack of selective affinity for cancer cells. Despite these limitations, phytochemicals remain essential in the eco-friendly fabrication of nanoparticles, offering a sustainable and promising approach for biomedical applications [8].

Curcumin (Cur), a naturally occurring polyphenol derived from Curcuma longa, has gained significant scientific interest due to its well-documented therapeutic properties. Curcumin exhibits a wide range of biological activities, including anti-inflammatory, antifungal, antioxidant, antibacterial, and anticancer effects. However, its therapeutic efficacy is restricted by poor solubility, rapid systemic metabolism, and low bioavailability, limiting its effectiveness in vivo [9,10]. To address these challenges, nanotechnology-based strategies have been explored to enhance curcumin's dissolution, stability, and absorption while maintaining its medicinal effectiveness. Encapsulation of curcumin within biogenic AgNPs offers a promising approach to overcoming these limitations, improving its pharmacokinetic profile, and enhancing its anticancer potential [11].

Folate-targeted drug delivery systems (DDS) have been extensively investigated for cancer therapy. Numerous studies have demonstrated the effectiveness of folic acid as a targeting ligand to facilitate site-specific drug delivery. The folate receptor (FR) is a membrane-bound glycoprotein that facilitates folate uptake through endocytosis and is overexpressed in many cancerous cells while showing minimal presence in normal cells. Specifically, FRα is highly expressed in rapidly growing malignancies, including breast, ovarian, lung, colon, and epithelial tumors [12,13]. The high FRα expression in cancer cell lines, such as MCF-7, highlights the potential of folate-conjugated nanoparticles for precise drug delivery, enhancing efficacy and minimizing unintended effects. Functionalization of AgNPs with folic acid enables targeted delivery of curcumin to breast cancer cells, improving selective cytotoxicity while reducing off-target effects on healthy tissues [14].

In this study, we propose a novel therapeutic approach by synthesizing AgNPs using H. cordata aqueous extract, followed by curcumin conjugation. The resulting bioactive compound–silver nanoparticle conjugate (Hc-AgNPs) was further functionalized with folic acid to enable precise targeting of folate receptors in breast cancer cells [15]. The integration of curcumin into the AgNPs enhances drug bioavailability, while folic acid facilitates targeted delivery to tumor sites, improving therapeutic efficacy and minimizing systemic toxicity. This study aims to synthesize and characterize H. cordata-mediated biogenic AgNPs co-loaded with curcumin and conjugated with folic acid (FA-Cur-Hc-AgNPs), evaluating their anticancer potential against breast cancer cells. The synergistic combination of biogenic AgNPs, curcumin, and folic acid offers a novel nanotherapeutic strategy for improved breast cancer treatment [16].

This research will focus on several key aspects, including nanoparticle characterization, cytotoxicity analysis, apoptosis induction, and drug release mechanisms, to establish the efficacy of FA-Cur-Hc-AgNPs as a targeted breast cancer therapy [17]. The study will investigate the physicochemical properties of the synthesized nanoparticles using advanced characterization techniques such as UV-Vis spectroscopy, Fourier-transform infrared spectroscopy (FTIR), scanning electron microscopy (SEM), and transmission electron microscopy (TEM). The in vitro anticancer potential of FA-Cur-Hc-AgNPs will be assessed using MTT assays to evaluate cytotoxicity against breast cancer cell lines, along with apoptosis assays to determine the mechanism of cell death induction [18].

Overall, this study aims to provide valuable insights into the development of biogenic AgNP-based targeted drug delivery systems for breast cancer treatment. By leveraging the synergistic effects of H. cordata-mediated AgNPs, curcumin, and folic acid, this research seeks to establish an effective and biocompatible nanotherapeutic approach to address the limitations of conventional cancer treatments.

2. MATERIALS AND METHODS

Materials

Silver nitrate, folic acid, curcumin, N-hydroxysuccinimide, sodium dihydrogen phosphate, Ethyl dimethylaminopropyl carbodiimide, NaOH, PEG 2000 and potassium dihydrogen phosphate were procured from Sigma-Aldrich. Milli-Q water, purged with nitrogen, was used in all steps of the synthesis and formulation of green silver nanoparticles. All the chemicals utilized in this study were of analytical grade, ensuring high purity and reliability for accurate experimental results.

Methods

Selection of Biological Source for Biogenic AgNP Synthesis

Houttuynia cordata (Hc) was sourced from NEDFi, Assam, to ensure authenticity and quality. For extract preparation, 10 g of powdered H. cordata was immersed in 100 mL of distilled water and subjected to Soxhlet extraction at 80 °C for 50 minutes, enabling efficient recovery of bioactive compounds through continuous solvent circulation. The resulting aqueous extract was filtered using Whatman No. 1 filter paper to eliminate insoluble particles, yielding a clear solution. To maintain stability and bioactivity, the extract was stored at 4 °C for further experimental use [19].

Synthesis of Biogenic AgNPs

The aqueous extract of Houttuynia cordata was mixed with 1 mM silver nitrate ($AgNO_3$) in varying volume ratios (Table 1) and continuously stirred at 1080 rpm for 3 hours at 50 °C. The formation of Hc-AgNPs was indicated by a characteristic dark brown color change. The synthesized nanoparticles were then separated by centrifugation at 15,000 rpm for 25 minutes. To remove unreacted or loosely bound molecules, the collected nanoparticles were thoroughly washed with ethanol and acetone. Finally, the purified Hc-AgNPs were dried to obtain a fine powder. [20-22].

Loading of Curcumin onto Biogenic AgNPs

To facilitate curcumin (Cur) loading, Hc-AgNPs (20 mg/mL in distilled water) were initially mixed with 10 mg of thiol-polyethylene glycol-amine ($HS\text{-}PEG_2K\text{-}NH_2$) and sonicated for 1 hour to ensure uniform dispersion. The solution was then kept undisturbed at room temperature for 24 hours to allow surface coating and ligand exchange between Hc-AgNPs and PEG [23].

Subsequently, a curcumin solution (20 mg/mL) was prepared by dissolving curcumin in 20 mL of phosphate-buffered saline (PBS) containing 0.05 N sodium hydroxide. This solution was added to the PEGylated Hc-AgNPs (PEG–Hc-AgNPs) and subjected to 20 minutes of sonication without heat to facilitate binding. The mixture was then incubated in the dark at 4 °C for 24 hours to enable efficient interaction between curcumin and PEG–Hc-AgNPs.

To eliminate any unbound molecules, the conjugate underwent three rounds of centrifugation at 18,000 rpm for 45 minutes. The obtained pellet was resuspended in sterile distilled water and further purified through an additional three rounds of centrifugation. Finally, the purified curcumin-conjugated nanoparticles (Cur–PEG–Hc-AgNPs) were stored at 4 °C for subsequent folic acid conjugation. [24].

Surface Modification of Curcumin-Loaded Biogenic AgNPs

To enhance the targeting capability, Cur–PEG–Hc-AgNPs were functionalized with folic acid (FA). For this modification, 10 mg of Cur–PEG–Hc-AgNPs was dispersed in 20 mL of an aqueous alkaline solution and stirred continuously for 1 hour to facilitate effective surface activation. Following this, 200 µL of ethyl dimethylaminopropyl carbodiimide (EDC) and 200 µL of N-hydroxysuccinimide (NHS) were gradually added dropwise to activate the carboxyl groups of folic acid for efficient conjugation. Subsequently, 5 mL of folic acid solution in an alkaline medium was introduced and mixed thoroughly to enable successful attachment to the nanoparticle surface [25]. To remove any unreacted components, the modified nanoparticles were centrifuged at 4000 rpm for 30 minutes. The supernatant was discarded, and the purified nanoparticles were lyophilized for 15–18 hours before being stored at 8°C for future applications. The bioactive compound profiles of H. cordata extract, Cur–PEG–Hc-AgNPs, and FA–Cur–PEG–Hc-AgNPs were quantitatively assessed using standard methods to determine total phenolic and flavonoid content. Additionally, the concentration of surface-bound folate on Cur–PEG–Hc-AgNPs was measured to confirm successful functionalization. [26].

Characterization of Folic acid functionalized curcumin loaded biogenic AgNPs

The physicochemical and morphological properties of H. cordata extract, Hc-AgNPs, and FA–Cur–PEG–Hc-AgNPs were analyzed using standard nanomaterial characterization techniques.

a) UV-Vis Spectroscopy:

The surface plasmon resonance (SPR) of the synthesized nanoparticles was confirmed using a UV-Vis spectrophotometer, revealing a characteristic absorption peak. The presence of an SPR peak at 366 nm for silver nanoparticles indicated successful synthesis and stability [27].

b) Particle Size, Polydispersity Index (PDI), and Zeta Potential:

Nanoparticle stability, uniformity, and surface charge were assessed using a Zetasizer. A lower PDI suggested uniform particle distribution, while zeta potential measurements provided insights into colloidal stability, crucial for optimizing drug delivery efficiency [28].

c) Fourier Transform Infrared Spectroscopy (FT-IR):

FT-IR analysis (PerkinElmer, USA) was conducted to examine molecular interactions between plant metabolites, silver nitrate, Hc-AgNPs, conjugated curcumin, and folic acid-functionalized Cur–Hc-AgNPs. This analysis helped confirm functional group modifications and successful ligand attachment [29].

d) Transmission Electron Microscopy (TEM):

To investigate nanoparticle morphology, size, and distribution, TEM (JEM-2100F, Japan) was employed. TEM provided high-resolution images essential for evaluating nanoparticle stability, internal structures, and surface modifications, all of which are critical for targeted drug delivery applications [30,31].

e) Scanning Electron Microscopy (SEM):

The surface topography and structural features of the synthesized nanoparticles were analyzed using SEM (JEOL-JSM 1200EX, Japan), providing further insights into their shape and surface characteristics, which play a key role in biomedical and pharmaceutical applications [32].

In-Vitro Cytotoxicity and Apoptosis Studies

The in-vitro cytotoxicity assessment of FA–Cur–Hc-AgNPs was conducted through an MTT assay, outsourced to Mr. Biologist, CRO, Guwahati, Assam, to evaluate the viability of breast cancer cell lines [33,34].

MTT Assay for Cell Viability

Breast cancer cells were cultured in Dulbecco's Modified Eagle Medium (DMEM) supplemented with 10% (v/v) fetal bovine serum (FBS) and maintained under standard conditions (37°C, 5% CO_2). The culture medium was refreshed every 2–3 days to ensure optimal growth. Upon reaching the required confluency, the cells were seeded into a 96-well plate and incubated with the test samples. Untreated cells served as the control. After 24 hours of incubation, the culture medium was removed, and the MTT reagent was added to each well. The plates were further incubated for 4 hours under the same conditions, allowing viable cells to metabolize MTT into formazan crystals. Subsequently, 100 µL of solubilization solution was introduced to dissolve the crystals, and the absorbance was recorded at 570 nm using a microplate reader. Cell viability (%) was calculated by comparing the absorbance of treated samples with that of the control [35].

Apoptosis Study Using AO-EtBr Staining

To assess apoptotic changes induced by FA–Cur–Hc-AgNPs, the Acridine Orange-Ethidium Bromide (AO-EtBr) dual staining technique was employed. Post-treatment, cells were examined under a fluorescence microscope. Acridine Orange (AO) binds to the DNA of viable cells with intact membranes, emitting green fluorescence, indicating healthy cells. Ethidium Bromide (EtBr) selectively stains non-viable and late apoptotic cells, producing an orange-red fluorescence, signifying apoptotic or necrotic cells. This staining method effectively differentiates normal, apoptotic, and necrotic cells based on fluorescence emission, providing insight into the cytotoxic and apoptotic effects of FA–Cur–Hc-AgNPs. [36-37].

3. RESULT

Numerous investigations have highlighted the potential of bioactive plant compounds and phytogenic metal nanoparticles (NPs) as promising candidates for alternative and adjunctive therapies. However, optimizing their pharmacological properties through nanotechnological interventions remains a critical area of research. In this context, folic acid and starch were employed as surface-functionalization agents to improve the anticancer potency of Hc-AgNPs, which were biosynthesized using an aqueous extract of Houttuynia cordata.

Fabrication and physicochemical analysis of folic acid-conjugated curcumin-loaded Houttuynia cordata-mediated silver nanoparticles (FA-Cur-HcAgNPs)

In this study, Houttuynia cordata extract and silver nitrate ($AgNO_3$) were employed for the green synthesis of folic acid- and curcumin-functionalized silver nanoparticles (FA-Cur-HcAgNPs). Various extract-to-metal precursor ratios (1:4, 1:8, 2:4, 2:8, and 3:5) were investigated to optimize nanoparticle formation, which was initially confirmed through UV-visible spectroscopy. The synthesized nanoparticles exhibited a distinct surface plasmon resonance (SPR) peak at 360 nm. A noticeable color transition from green to dark brown further validated the reduction of $AgNO_3$ and the successful formation of HcAgNPs. Among the tested formulations, the 1:4 Hc-$AgNO_3$ ratio demonstrated the most pronounced absorption peak at 350 nm, indicating efficient nanoparticle synthesis. Upon incorporation of curcumin and folic acid into Hc-AgNPs, the absorption peak underwent a slight shift to 340 nm, confirming the successful conjugation of the green-synthesized silver nanoparticles. This shift in wavelength further validated the effective incorporation of curcumin and folic acid into the Hc-AgNPs.

Determination of nanoparticle size distribution and surface charge characteristics

Zeta potential analysis is a crucial technique in nanomaterials research for evaluating particle size, distribution, polydispersity index (PDI), and surface charge, all of which influence the stability and bioavailability of nanoparticles. For efficient nanotherapeutics, an ideal particle size below 200 nm and a PDI less than 0.2 are preferred to enhance systemic circulation, dispersion, and therapeutic efficacy (**Figure 1)**.

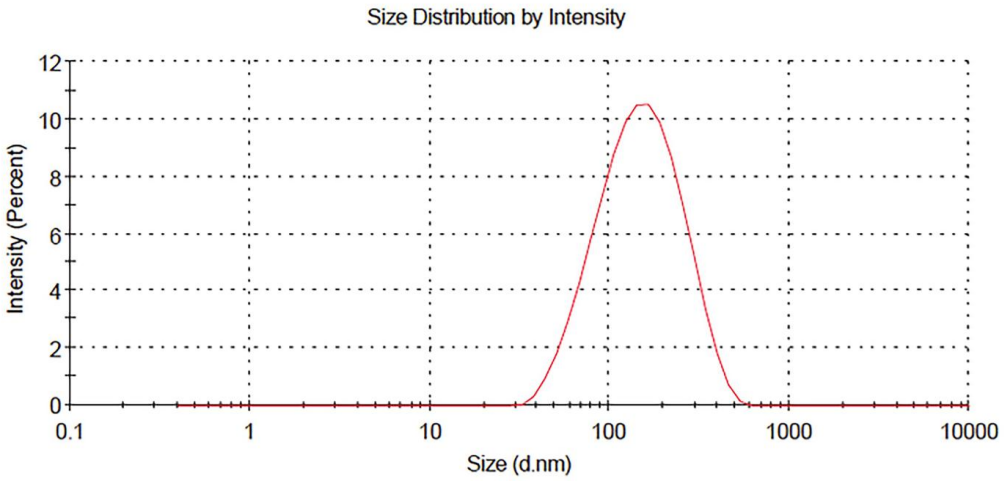

Figure 1: Particle Size analysis of FA-Cur-Hc-AgNPs

In this study, the size, zeta potential, and PDI of Houttuynia cordata-mediated silver nanoparticles (HcAgNPs) were systematically optimized before and after functionalization with aminated curcumin and folic acid **(Table 1).** HcAgNPs were synthesized using different extract-to-$AgNO_3$ ratios (1:4, 1:8, 2:4, 2:8, and 3:5), with increasing silver nitrate concentrations leading to larger particle sizes.

Table 1. Particle size, zeta potential and poly dispersity index of FA-Cur-Hc-AgNPs in different ratio of Hc-Cur-AgNPs and FA-Cur-Hc-AgNPs.

Formulations	Conjugation ratio (v/v)	Particle size (nm±SD)	Zeta potential (mV±SD)	PDI±SD
Hc-AgNPs (Hc: AgNO3)	1:4	158.21±1.12	-33.51±0.12	0.188±0.12
	1:8	224.54±1.05	-47.62±0.23	0.395±0.04
	2:4	278.31±0.76	-21.71±0.32	0.243±0.02
	2:8	385.23±0.22	-25.35±0.16	0.412±0.06
	3:5	486.62±0.54	-9.92±0.11	0.541±0.03
Cur-Hc-AgNPs (Cur:Hc-AgNPs)	9:1	184.21±0.07	-39.72±0.07	0.224±0.16
	8:2	137.43±1.14	-44.61±0.22	0.354±0.13
	7:3	294.52±1.02	-23.71±0.13	0.397±0.11
	6:4	416.34±0.54	-9.64±0.16	0.678±0.08
FA-Cur-Hc-AgNPs FA: Cur-Hc-AgNPs	2:8	176.24±1.53	-41.33±1.12	0.156±0.21

The optimized 1:4 formulation exhibited an average particle size of 158.21 nm, a PDI of 0.188, and a zeta potential of –33.51 mV, ensuring colloidal stability **(Figure 2).**

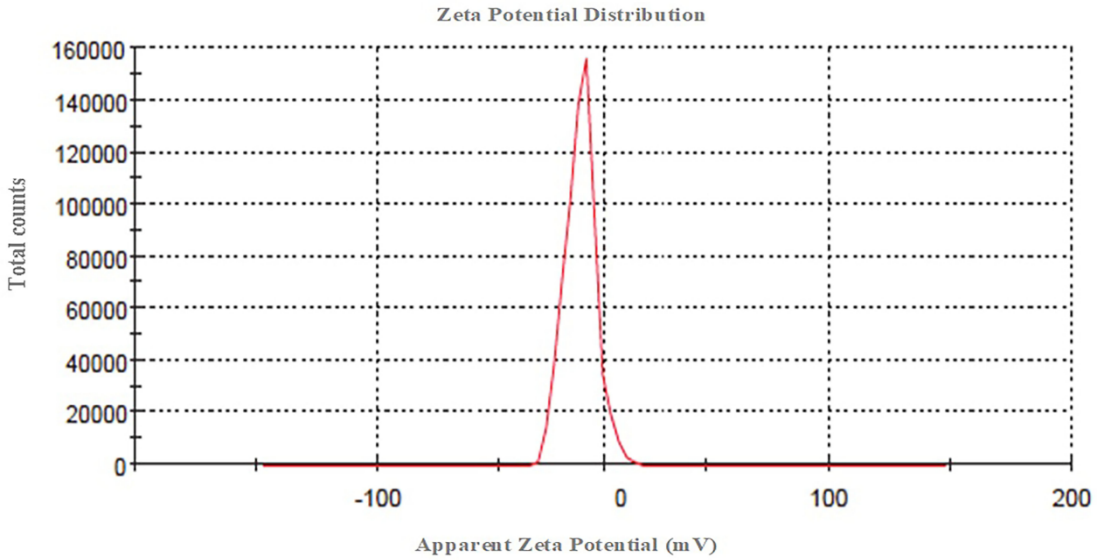

Figure 2: Zeta potential analysis of FA-Cur-Hc-AgNPs

Upon conjugation with curcumin at a 9:1 ratio, the nanoparticles increased in size to 184.21 nm, with a PDI of 0.224 and a zeta potential of –39.72 mV. The structural stability and charge distribution of FA-Cur-HcAgNPs were attributed to (i) amine-functionalized curcumin acting as a capping agent for the green-synthesized AgNPs and (ii) folic acid conjugation via EDC/NHS-mediated coupling, which facilitated amide bond formation between free amine groups. This modification significantly enhanced the positive surface charge of the nanoparticles, promoting strong electrostatic interactions with negatively charged cancer cell membranes. Consequently, the increased cellular uptake of FA-Cur-HcAgNPs highlights their potential as a targeted drug delivery platform for improved anticancer efficacy.

Fourier Transform Infrared (FT-IR) Spectroscopic Characterization

Fourier Transform Infrared (FT-IR) spectroscopy was employed to characterize Houttuynia cordata extract, biosynthesized HcAgNPs, curcumin, folic acid, and the final FA-Cur-HcAgNPs formulation within the spectral range of 4000–500 cm^{-1} **(Figure 3).**

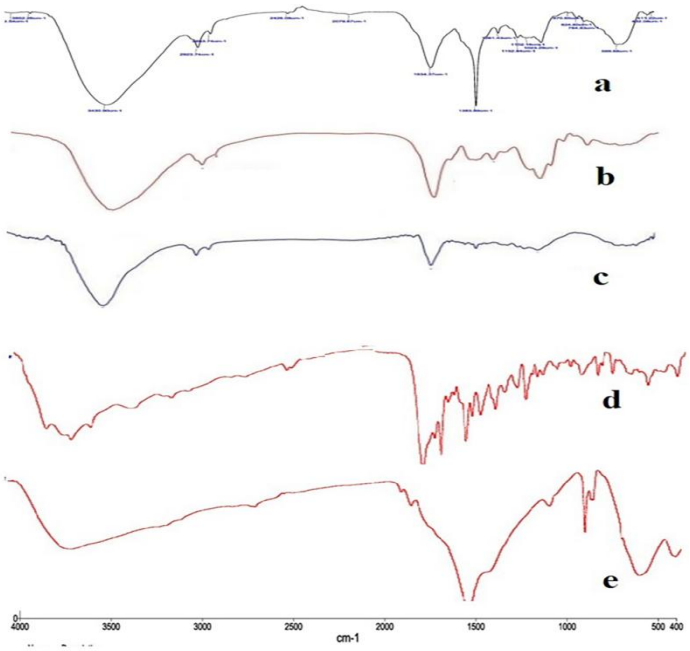

Figure 3. FT-IR spectra of (a) H. cordata plant extract, (b) Silver (c) Curcumin (d) Folic acid and (e) FA-Cur-Hc-AgNPs

The FT-IR spectrum of H. cordata extract exhibited distinct peaks corresponding to O–H stretching (hydroxyl and phenolic groups), N–H stretching (amine groups), C–H stretching (aliphatic and aromatic compounds), C=O stretching (carbonyl groups from flavonoids and ketones), C=C stretching (aromatic systems and flavonoids), and C–O stretching (phenols and carbohydrates). The $AgNO_3$ spectrum displayed characteristic absorption bands for N–O asymmetric and symmetric stretching (NO_3^- group) and O–Ag vibrations.

Curcumin exhibited absorption bands for O–H stretching, C=O stretching (β-diketone and conjugated carbonyl groups), C=C stretching (aromatic system), and C–O–C stretching (ether linkage). Similarly, folic acid demonstrated characteristic peaks corresponding to O–H stretching (carboxyl group), N–H stretching (amide and amine groups), C=O stretching (carboxyl and amide groups), C=N stretching (pteridine ring system), and C–H bending (aromatic moieties).

The FT-IR spectrum of FA-Cur-HcAgNPs confirmed successful functionalization through notable spectral shifts. Broadening of the O–H and N–H stretching bands in the range of 3400–3200 cm^{-1} indicated strong hydrogen bonding and biomolecular interactions with AgNPs. The shift of the C=O stretching peak (from 1700 cm^{-1} to 1650 cm^{-1}) suggested effective conjugation of curcumin and folic acid onto the nanoparticle surface. The presence of additional peaks corresponding to C=N (pteridine ring), C=C (aromatic system), and C–O (phenolics, ether linkages, and carbohydrates) further validated the successful functionalization. Furthermore, new absorption bands appearing around 500–450 cm^{-1} confirmed Ag–O and Ag–N interactions, substantiating the formation of nanoparticles and their biomolecule binding. These findings collectively demonstrate the effective synthesis, functionalization, and stabilization of FA-Cur-HcAgNPs, reinforcing their potential in targeted drug delivery applications.

Transmission Electron Microscopy (TEM) and Scanning Electron Microscopy (SEM) Characterization

Transmission electron microscopy (TEM) and scanning electron microscopy (SEM) were utilized to analyze the structural morphology, particle size, and surface characteristics of HcAgNPs and FA-Cur-HcAgNPs **(Figure 4).**

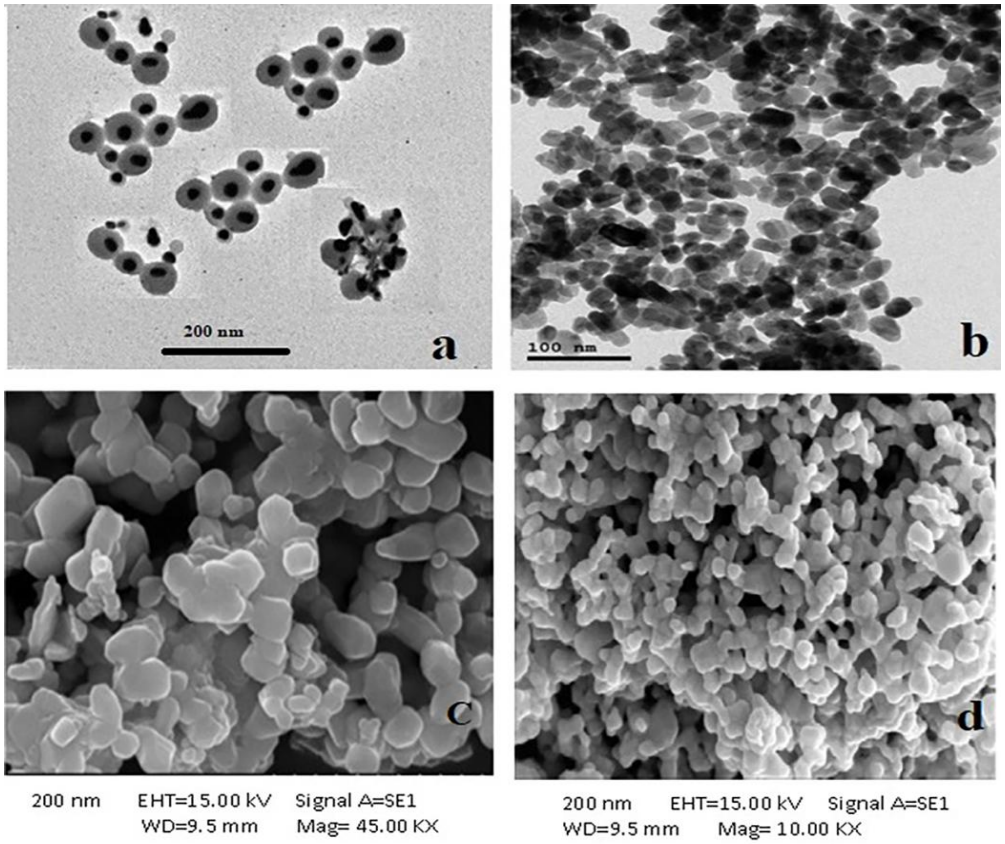

Figure 4. TEM (a,b) and SEM (c,d) images of FA-Cur-Hc-AgNPs

The particle size of Hc-AgNP at different ratio was ranged from 158.21 to 486.62 nm. In contrast, Cur-Hc-AgNPs exhibited the particle size range of 121.42 nm, with a particle distribution ranging from 184.21 to 416.34 nm. The SEM images demonstrated the formation of multilayered nanostructures with predominantly hexagonal and oval-shaped morphologies. The observed nanoparticle aggregation was likely influenced by biomolecules from the plant extract, which acted as capping agents. Furthermore, the structural analysis confirmed the successful functionalization of the synthesized nanoparticles with curcumin and folic acid, validating their effective conjugation within the nanoformulation.

Results of MTT assay and cell apoptosis

The MTT assay findings demonstrated that FA-Cur-HcAgNPs exhibited potent cytotoxic activity against MCF-7 breast cancer cells, with a progressive increase in cell inhibition over time **(Table 2)**. At 0 hours, all groups exhibited a dense monolayer of cells, indicating a uniform initial cell population before treatment.

Table 2. Results of MTT assay and percentage of cell survival

Conc. (PPM)	**Absorbance**			**Average**	**% Cell Survival**			**Average% cell Survival**
Control (CTRL)	1.118	1.407	1.115	1.213	92.14	115.96	91.90	100.00
750	0.971	1.017	1.188	1.059	80.03	83.82	97.91	87.25
1500	1.307	1.143	1.056	1.169	107.72	94.20	87.03	96.32
3750	0.925	1.028	0.986	0.980	76.24	84.73	81.26	80.74
7500	0.47	0.306	0.67	0.482	38.74	25.22	55.22	39.73
15000	0.436	0.171	0.452	0.353	35.93	14.09	37.25	29.09
IC50 Value	5313.34							

By 12 hours, a noticeable reduction in cell density was observed in the FA-Cur-Hc-AgNP treated group, suggesting the early onset of apoptosis or cytotoxic effects. At 24 hours, substantial cell death was evident, highlighting the enhanced therapeutic efficacy of FA-Cur-Hc-AgNPs, likely attributed to folic acid functionalization, which facilitates targeted uptake by folate receptor-overexpressing MCF-7 cells **(Figure 5).** In comparison, Cur-Hc-AgNPs and Hc-AgNPs also induced cytotoxic effects but to a lesser degree, while the blank nanoparticle group showed minimal impact, confirming the role of curcumin and silver nanoparticles in inducing cell death. These findings underscore the potential of FA-Cur-Hc-AgNPs as a promising targeted nanotherapeutic approach for breast cancer treatment.

The AO/EtBr staining assay images demonstrate the cytotoxic and apoptotic effects of folic acid-functionalized, curcumin-loaded, biogenically synthesized silver nanoparticles against breasr cancer cell lines. Blue channel represents nuclear staining which stains DNA and highlights cell nuclei. The red spots in the composite image indicate apoptotic or necrotic region. The colored areas (green) Indicate metabolically active cells. The coexistence of apoptotic (red) and viable (green) cells indicates a heterogeneous cell population, confirming that FA-Cur-HcAgNPs trigger apoptosis in MCF-7 cells **(Figure 6).** Acridine orange (AO) selectively stains viable and early apoptotic cells, emitting green fluorescence, whereas ethidium bromide (EtBr) preferentially penetrates late apoptotic and necrotic cells, resulting in red fluorescence. Additionally, blue fluorescence, likely from a nuclear stain such as DAPI, highlights nuclear morphology, allowing visualization of chromatin condensation and nuclear fragmentation-hallmarks of apoptosis. The observed shift from predominantly green fluorescence to increased red fluorescence over time suggests progressive apoptosis, with cells transitioning from an early apoptotic state to late-stage apoptosis or necrosis. The presence of condensed or fragmented nuclei further confirms apoptotic induction. These findings indicate the efficacy of FA-Cur-HcAgNPs in inducing apoptosis in MCF-7 cells, supporting their potential as targeted nanotherapeutics for breast cancer treatment.

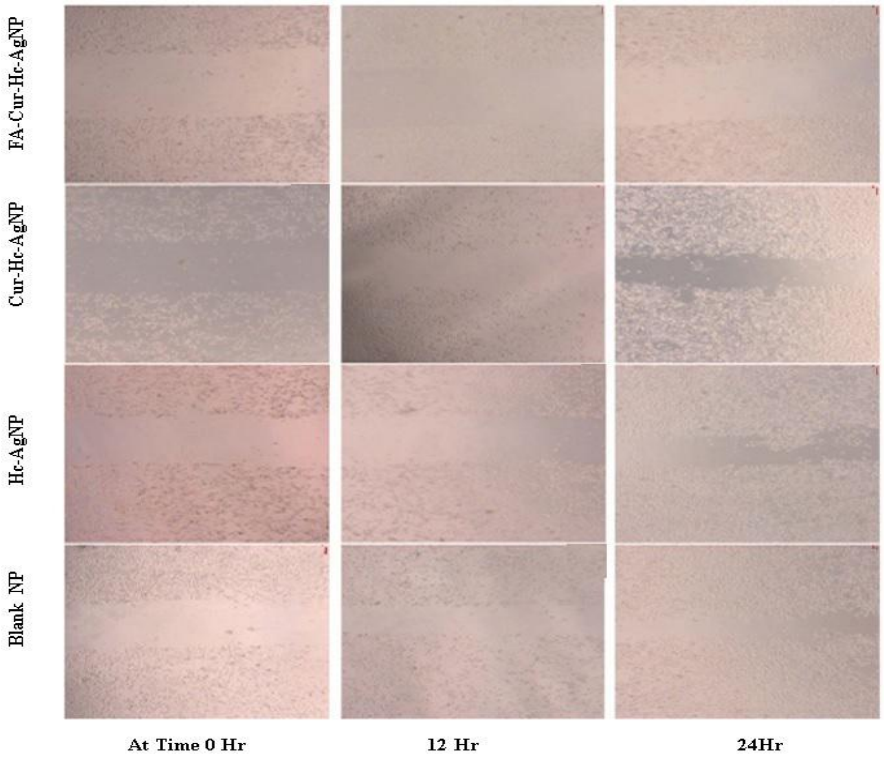

Figure 5. MTT assay of Blank NPs, Hc-AgNPs, Cur-Hc-AgNPs and FA-Cur-Hc-AgNPs

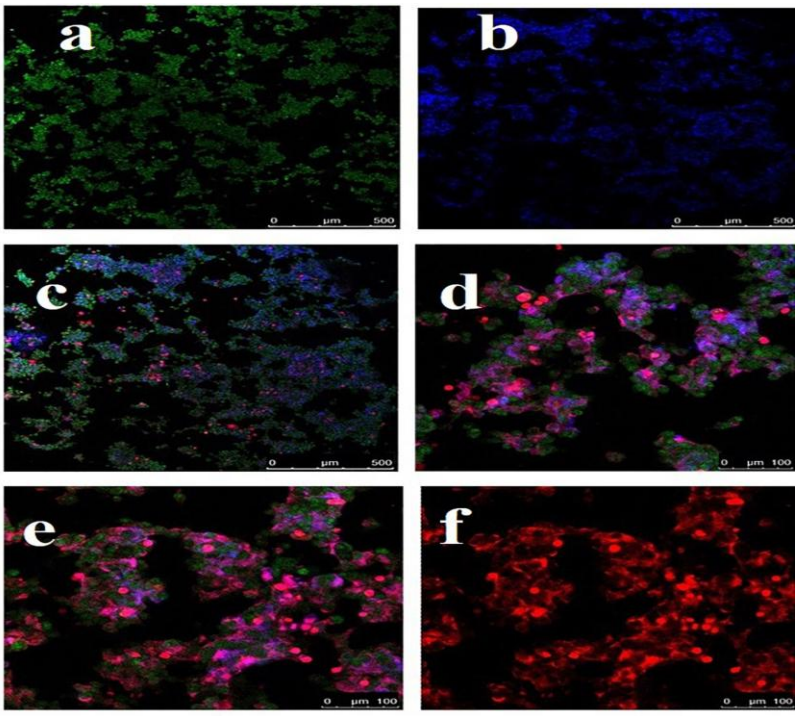

Figure 6. Cell apoptosis studies of FA-Cur-Hc-AgNPs on normal and cancer cells under low and high magnification.

(a) Green Image showing Annexin V-FITC, binds on the outer membrane of apoptotic cells (early apoptosis marker). (b) Blue image represents DAPI, which stains cell nuclei (c) Image showing early and late apoptosis or necrosis green (Annexin V), blue (DAPI), and red (Propidium Iodide - PI). (d) Image showing co-localization of signals. (e) Image shows detailed

visualization of cells. Pink/magenta areas likely indicate apoptotic or necrotic cells where red and blue signals overlap. (f) Image shows Propidium Iodide (PI) staining, which only penetrates cells with compromised membranes (late apoptosis/necrosis marker).

4. DISCUSSION

The study successfully synthesized and characterized folic acid- and curcumin-functionalized silver nanoparticles (FA-Cur-Hc-AgNPs) using an aqueous extract of Houttuynia cordata. UV-visible spectroscopy confirmed nanoparticle formation with a characteristic absorption peak shift, indicating successful conjugation of folic acid and curcumin. The finalized FA-Cur-HcAgNPs formulation exhibited a mean particle size of 184.21 nm, a polydispersity index (PDI) of 0.224, and a zeta potential of -39.72 mV. These properties confirm effective surface modification, ensuring enhanced colloidal stability and facilitating targeted cancer cell interactions via electrostatic forces. FT-IR analysis further validated the incorporation of biomolecules, With noticeable spectral alterations in functional groups hydroxyl, amine, carbonyl and imine, while new peaks in the 500–450 cm^{-1} range confirmed Ag-O and Ag–N interactions, supporting nanoparticle formation and stabilization. Morphological analysis using TEM and SEM revealed hexagonal and oval-shaped nanoparticles with some degree of agglomeration, likely due to plant extracts. Differences in particle size before and after functionalization further confirmed successful conjugation. Cytotoxicity assessment through the MTT assay demonstrated that FA-Cur-Hc-AgNPs exert significant time- and dose-dependent cytotoxic effects on cancer cell lines, exhibiting an IC_{50} value of 5313.34 ppm, indicating the concentration required for 50% cell inhibition. The FA-functionalized nanoparticles exhibited enhanced efficacy compared to non-functionalized Hc-AgNPs and Cur-Hc-AgNPs, likely due to folate receptor-mediated uptake by cancer cells. Over 24 hours, treated cells showed progressive viability reduction, confirming apoptosis induction and highlighting the potential of FA-Cur-Hc-AgNPs as targeted nanotherapeutics.

5. CONCLUSION

This study successfully synthesized and characterized folic acid- and curcumin-functionalized silver nanoparticles (FA-Cur-Hc-AgNPs) using an aqueous extract of *Houttuynia cordata*. The nanoparticles exhibited optimized physicochemical properties, with a mean particle diameter of 184.21 nanometer, a poly dispersity index of 0.224, and a surface charge measurement of -39.72 mV, contributing to enhanced stability and interaction with cancer cells. UV-visible spectroscopy and FT-IR analysis confirmed successful conjugation. Cytotoxicity studies of FA-Cur-HcAgNPs exhibited significant anticancer activity against breast cancer cell lines in a dose- and time-dependent manner. This suggests that increasing the nanoparticle concentration enhances cytotoxicity, likely due to increased cellular uptake and intracellular accumulation of bioactive compounds. Additionally, prolonged exposure duration allows for progressive nanoparticle interaction with cancer cells, leading to enhanced therapeutic efficacy. The half-maximal inhibitory concentration (IC_{50}) represents the concentration of FA-Cur-Hc-AgNPs required to inhibit 50% of cancer cell lines for breast cancer. An IC_{50} value of 5313.34 ppm suggests a notable cytotoxic effect, indicating the nanoparticles' therapeutic potential. The potency of the formulation can be attributed to the combined action of silver nanoparticles (AgNPs), curcumin, and folic acid, which work synergistically to induce cell death in MCF-7 cells. Thus, Biogenic silver nanoparticles co-loaded with curcumin and folic acid exhibit enhanced targeted cytotoxicity, synergistic anticancer effects, and reduced off-target toxicity, demonstrating a promising, green, and effective therapeutic strategy for breast cancer treatment.

6. ACKNOWLEDGEMENT

We sincerely extend our heartfelt gratitude to the Contract Research Organization, Mr. Biologist, Guwahati for facilitating the outsourcing of the MTT assay and cell apoptosis studies.

REFERENCES

[1] Visser LL, Groen EJ, van Leeuwen FE, Lips EH, Schmidt MK, Wesseling J. Predictors of an invasive breast cancer recurrence after DCIS: a systematic review and meta-analyses. Cancer Epidemiol Biomarkers Prev. 2019; 28(5):835-45. doi:10.1158/1055-9965.EPI-18-0976.

[2] Mariotto AB, Etzioni R, Hurlbert M, Penberthy L, Mayer M. Estimation of the number of women living with metastatic breast cancer in the United States. Cancer Epidemiol Biomarkers Prev. 2017;26(6):809-15. doi:10.1158/1055-9965.EPI-16-0889.

[3] Ghoncheh M, Pournamdar Z, Salehiniya H. Incidence, mortality and epidemiology of breast cancer in the world. Asian Pac J Cancer Prev. 2016;17(S3):43-6. doi:10.7314/apjcp.2016.17.s3.43.

[4] Britt KL, Cuzick J, Phillips KA. Key steps for effective breast cancer prevention. Nat Rev Cancer. 2020;11(1):1-20. doi:10.1038/s41568-020-0266-x.

[5] Ganesan K, Wang Y, Gao F, Liu Q, Zhang C, Li P, et al. Targeting engineered nanoparticles for breast cancer therapy. Pharmaceutics. 2021;13(11):1829. doi:10.3390/pharmaceutics13111829.

[6] Malik JA, Ansari JA, Ahmed S, Khan A, Ahemad N, Anwar S. Nano-drug delivery system: A promising

approach against breast cancer. Ther Deliv. 2023;14(6):357-81. doi:10.4155/tde-2023-0020.

[7] Sattari R, Khayati GR, Hoshyar R. Biosynthesis and characterization of silver nanoparticles capped by biomolecules by Fumaria parviflora extract and their cytotoxicity against MDA-MB-468 cell lines. Mater Chem Phys. 2019;241:122438. doi:10.1016/j.matchemphys.2019.122438.

[8] Saravanakumar K, Chelliah R, MubarakAli D, Oh DH, Kathiresan K, Wang MH. Unveiling the potentials of biocompatible silver nanoparticles on human lung carcinoma A549 cells and Helicobacter pylori. Sci Rep. 2019;9(1):1-8. doi:10.1038/s41598-019-42112-1.

[9] Mariadoss AVA, Vinayagam R, Xu B, Venkatachalam K, Sankaran V, Vijayakumar S, et al. Phloretin loaded chitosan nanoparticles enhance the antioxidant and apoptotic mechanisms in DMBA-induced experimental carcinogenesis. Chem Biol Interact. 2019;308:11-9. doi:10.1016/j.cbi.2019.05.008.

[10] Saravanan A, Senthil Kumar P, Karishma S, Vo DVN, Jeevanantham S, Yaashikaa PR, et al. A review on biosynthesis of metal nanoparticles and its environmental applications. Chemosphere. 2021;264(Pt 2):128580. doi:10.1016/j.chemosphere.2020.128580.

[11] Pradhan S, Rituparna S, Dehury H, Dhall M, Singh YD. Nutritional profile and pharmacological aspect of Houttuynia cordata Thunb. and their therapeutic applications. Pharmacol Res Mod Chin Med. 2023;9:100311. doi:10.1016/j.prmcm.2023.100311.

[12] Sun L, Liu H, Ye Y, Lei Y, Islam R, Tan S, et al. Smart nanoparticles for cancer therapy. Signal Transduct Target Ther. 2023;8(418):1-15. doi:10.1038/s41392-023-01642-x.

[13] Gomes HIO, Martins CSM, Prior JAV. Silver nanoparticles as carriers of anticancer drugs for efficient target treatment of cancer cells. Nanomaterials. 2021;11(4):964. doi:10.3390/nano11040964.

[14] Mariadoss AVA, Ramachandran V, Shalini V, Agilan B, Franklin JH, Sanjay K, et al. Green synthesis, characterization and antibacterial activity of silver nanoparticles by Malus domestica and its cytotoxic effect on MCF-7 cell line. Microb Pathog. 2019;135:103609.

[15] Padil VVT, Cernik M. Green synthesis of copper oxide nanoparticles using gum karaya as a biotemplate and their antibacterial application. Int J Nanomedicine. 2013;8:889. doi:10.2147/IJN.S40599.

[16] Ghoran SH, Calcaterra A, Abbasi M, Taktaz F, Nieselt K, Babaei E. Curcumin-based nanoformulations: A promising adjuvant towards cancer treatment. Molecules. 2022;27(16):5236. doi:10.3390/molecules27165236.

[17] Farani MR, Azarian M, Sheikh Hossein HH, Abdolvahabi Z, Abgarmi ZM, Moradi A, et al. Folic acid-adorned curcumin-loaded iron oxide nanoparticles for cervical cancer. ACS Appl Bio Mater. 2022;5(3):1258-71. doi:10.1021/acsabm.1c01311.

[18] Türkeş E, Sağ Açıkel Y. Folic acid-conjugated cancer drug curcumin-loaded albumin nanoparticles: Investigation of curcumin release kinetics. J Drug Deliv Sci Technol. 2024;91:105178. doi:10.1016/j.jddst.2023.105178.

[19] Cheng W, Nie J, Xu L, Liang C, Peng Y, Liu G, et al. pH-sensitive delivery vehicle based on folic acid-conjugated polydopamine-modified mesoporous silica nanoparticles for targeted cancer therapy. ACS Appl Mater Interfaces. 2017;9(23):18462-73. doi:10.1021/acsami.7b02457.

[20] Thulasidasan AKT, Retnakumari AP, Shankar M, Vijayakurup V, Anwar S, Thankachan S, et al. Folic acid conjugation improves the bioavailability and chemosensitizing efficacy of curcumin-encapsulated PLGA-PEG nanoparticles towards paclitaxel chemotherapy. Oncotarget. 2017;8(64):107374-89. doi:10.18632/oncotarget.22376.

[21] Parker N, Turk MJ, Westrick EW, Lewis JD, Low PS, Leamon CP. Folate receptor expression in carcinomas and normal tissues determined by a quantitative radioligand binding assay. Anal Biochem. 2005;338(2):284-93. doi:10.1016/j.ab.2004.12.026.

[22] Mansoori GA, Brandenburg KS, Shakeri-Zadeh A. A comparative study of two folate-conjugated gold nanoparticles for cancer nanotechnology applications. Cancers. 2010;2(4):1911-28. doi:10.3390/cancers2041911.

[23] Leone JP, Bhargava R, Theisen BK, Hamilton RL, Lee AV, Brufsky AM. Expression of high-affinity folate receptor in breast cancer brain metastasis. Oncotarget. 2015;6(30):30327-33. doi:10.18632/oncotarget.4639.

[24] Nawaz FZ, Kipreos ET. Emerging roles for folate receptor FOLR1 in signaling and cancer. Trends Endocrinol Metab. 2022;33(3):159-74. doi:10.1016/j.tem.2021.12.003.

[25] Zhang Z, Wang J, Tacha DE, Li P, Bremer RE, Chen H, et al. Folate receptor α associated with triple-negative breast cancer and poor prognosis. Arch Pathol Lab Med. 2014;138(7):890-5. doi:10.5858/arpa.2013-0309-OA.

[26] Nawaz FZ, Kipreos ET. Emerging roles for folate receptor FOLR1 in signaling and cancer. Trends Endocrinol Metab. 2022;33(3):159-74. doi:10.1016/j.tem.2021.12.003.

[27] Zhang Z, Wang J, Tacha DE, Li P, Bremer RE, Chen H, et al. Folate receptor α associated with triple-negative breast cancer and poor prognosis. Arch Pathol Lab Med. 2014;138(7):890-5. doi:10.5858/arpa.2013-0309-OA.

[28] Sathiyaseelan K, Saravanakumar K, Mariadoss AVA, Wang MH. Biocompatible fungal chitosan encapsulated phytogenic silver nanoparticles enhanced antidiabetic, antioxidant and antibacterial activity. Int J Biol Macromol. 2020;153:63-71. doi:10.1016/j.ijbiomac.2020.02.291.

[29] Butzbach K, Konhäuser M, Fach M, Bamberger DN, Breitenbach B, Epe B, et al. Receptor-mediated uptake of folic acid-functionalized dextran nanoparticles for applications in photodynamic therapy. Polymers (Basel). 2019;11(5):896. doi:10.3390/polym11050896.

[30] Hasan SS, Singh S, Parikh RY, Dharne MS, Patole MS, Prasad B, et al. Bacterial synthesis of copper/copper oxide nanoparticles. J Nanosci Nanotechnol. 2008;8(6):3191-6. doi:10.1166/jnn.2008.095.

[31] Danaei M, Dehghankhold M, Ataei S, Hasanzadeh Davarani F, Javanmard R, Dokhani A, et al. Impact of particle size and polydispersity index on the clinical applications of lipidic nanocarrier systems. Pharmaceutics. 2018;10(2):57. doi:10.3390/pharmaceutics10020057.

[32] Danaei M, Dehghankhold M, Ataei S, Hasanzadeh Davarani F, Javanmard R, Dokhani A, et al. Impact of particle size and polydispersity index on the clinical applications of lipidic nanocarrier systems. Pharmaceutics. 2018;10(2):57. doi:10.3390/pharmaceutics10020057.

[33] Stati G, Rossi F, Trakoolwilaiwan T, Tung LD, Mourdikoudis S, Thanh NTK, et al. Development and characterization of curcumin-silver nanoparticles as a promising formulation to test on human pterygium-derived keratinocytes. Molecules. 2022;27(1):282. doi:10.3390/molecules27010282.

[34] Dutta D, Pajaniradje S, Nair AS, Chandramohan S, Bhat SA, Manikandan E, et al. An in vitro study of active targeting and anti-cancer effect of folic acid-conjugated chitosan-encapsulated indole curcumin analogue nanoparticles. Int J Biol Macromol. 2024;282(Pt 5):136990. doi:10.1016/j.ijbiomac.2024.136990.

[35] Liu JL, Pan YY, Chen O, Luan Y, Xue X, Zhao JJ, et al. Curcumin inhibits MCF-7 cells by modulating the NF-κB signaling pathway. Oncol Lett. 2017;14(5):5581-4. doi:10.3892/ol.2017.6860.

[36] Saharkhiz S, Zarepour A, Zarrab A. Empowering cancer therapy: Comparing PEGylated and non-PEGylated niosomes loaded with curcumin and doxorubicin on MCF-7 cell line. Bioengineering (Basel). 2023;10(10):1159. doi:10.3390/bioengineering10101159.

[37] Raphael R, Aswathy WF, Anila EI. In vitro cytotoxicity studies of Ga_2O_3 microstructures on L929 and MCF-7 cell lines using MTT assay. MRS Commun. 2024;14(6):1359-63. doi:10.1557/s43579-024-00647-z..